International Journal of Environmental Science and Technology (2019) 16:113–124
https://doi.org/10.1007/s13762-018-1647-5

ORIGINAL PAPER

Effect of thermal regeneration of diatomite adsorbent on its efficacy for removal of dye from water

H. Aguedal[1] · A. Iddou[1] · A. Aziz[1] · A. Shishkin[2] · J. Ločs[2] · T. Juhna[3]

Received: 8 February 2017 / Revised: 10 June 2017 / Accepted: 3 January 2018 / Published online: 18 January 2018

Abstract
Reduction in adsorption capacities of adsorbents is limiting of its wider application for water treatment. In this study, we developed a new approach for recycling diatomite to be used adsorbent. The laser scattering particle size analyzer, X-ray diffraction, scanning electron microscopy/energy-dispersive X-ray and Brunauer–Emmett–Teller analysis were used to evaluate the structural characteristics of treated samples. The adsorption efficacy of raw and heated diatomite at 300, 600 and 900 °C for textile dyestuff removal from wastewater was investigated. The characterization results show insignificant changes except some deconstructions were occurred after treatment at 900 °C. The maximum adsorption capacities were obtained at pH 2 and adsorbent dosage of 4 g L^{-1}. The required time to reach the equilibrium was 30 min, and diatomite treated at 600 °C is acted as an excellent adsorbent. The kinetic studies were better described by the pseudo-second-order kinetic model. The isotherms experimental data showed that the adsorption of dye onto raw diatomite, DH300 and DH600 follows the Brunauer–Emmett–Teller isotherm model, but its adsorption onto DH900 conforms well to Freundlich isotherm model. Recycling of diatomite using thermal treatment was useful. At 600 °C which is considered the best regeneration temperature, the adsorbed dye was completely despaired, and around 73% was restored after three regeneration cycles.

Keywords Diatomite · Dye adsorption · Thermal regeneration · Wastewater purification

Introduction

Synthetic dyes are widely used by different industries such as textile, rubber, leather tanning, paper, printing, cosmetics, food. Around 10,000 types of commercial dyes and more than 0.7 million tons of synthetic dyes are produced annually in worldwide (Mahmoodi et al. 2011). This wide use of dyes in daily life has produced enormous volumes of effluents containing dyestuff and poses considerable management problems in wastewater industry. Around 15% of synthetic dyes used are lost during production and improper processing (Mahmoodi and Arami 2008). Even at low concentrations, these pollutants reduce the sunlight penetration, affecting thereby the process of photosynthesis which destroys the food webs and aquatic life existing in water ecosystem. Human health is threatened not only by the toxicity, carcinogenic, and mutagenic effect of these contaminants, but also by the incorporation of some dyes in food products which may cause asthma, urticarial, eczema and allergic reactions in humans bodies (Wang et al. 2006).

The presence of dyes in environment has become one of the most difficult problems to solve in developing countries. Due to their complex structure and non-biodegradability behavior providing a high stability and resistant to light and oxidative agents complicates the choice of appropriate method for their treatment (Devi et al. 2015). Several wastewater technologies have been used to remove dyes including coagulation/flocculation, advanced oxidation processes,

Editorial responsibility: M. Abbaspour.

✉ H. Aguedal
hakim.aguedal@gmail.com

[1] Laboratoire de Valorisation des Matériaux, Département de Génie des Procédés, Faculté des Sciences et de la Technologie, Université Abdelhamid Ibn Badis – Mostaganem, Bp. 227, 27000 Mostaganem, Algeria

[2] Rudolfs Cimdins Riga Biomaterials Innovations and Development Centre of RTU, Institute of General Chemical Engineering, Faculty of Materials Science and Applied Chemistry, Riga Technical University, Pulka 3, Riga 1007, Latvia

[3] Laboratory of Water Research, Faculty of Civil Engineering, Riga Technical University, Ķīpsalas iela 6a -263, Riga 1048, Latvia

ozonation, membrane separation, electrochemical methods, adsorption on activated carbon and biological treatment (Akar et al. 2009; Belala et al. 2011). However, these technologies are expensive because of capital costs investments, extensive energy and chemicals use (Reddad et al. 2002). In contrast, the adsorption technology has been proven to be advantageous because of less investment cost, easy and simple design operations, no toxic by-products and possibilities of adsorbents regeneration and adsorbate recovery (Mittal et al. 2009).

The selection of adsorbent material is still the main concern in this technique. It is known that the activated carbon is widely used adsorbent due to its high surface capacity and low specificity in respect to properties of pollutants (Chen et al. 2013; Djilani et al. 2015). However, due to higher costs of its synthesis and regeneration activated carbon is difficult to afford by industry in the developing countries (Vimonses et al. 2009a). In recent years, the development of low-cost adsorbents from different locally available materials has attracted considerable attentions of scientific researchers. A wide variety of adsorbents material has been experimented and tested for dyestuff and heavy metals removing from wastewater such as agro waste products (Aziz et al. 2009; Bhatti and Nausheen 2014), sludge from wastewater treatment (Iddou and Ouali 2008), algae biomass (Iddou et al. 2011), biosorbents as: bacteria, yeasts and fungi (Djafer et al. 2014; Kelewou et al. 2014), clay and mineral materials (de Sales et al. 2013; Abidi et al. 2015).

Diatomite is natural aluminosilicate mineral material, which largely consists of fossilized skeletons of unicellular aquatic plants found in sedimentary rocks. It is readily available and low-cost materials of variety of shape and size generally ranging between 10 and 200 µm (Yuan et al. 2010). Many of physical and chemical characteristics, such as highly porous structure, low density, high surface area and low thermal conductivity, lead to use it as filter in water purification, as sound and thermal insulation in building construction, as catalyst support in semiconductors materials, etc. (Wang et al. 2015). Therefore, diatomite has been used successfully as adsorbent in wastewater treatment to remove pollutants such as heavy metals (Ye et al. 2015) and dyes (Sheshdeh et al. 2014).

It was reported that some of these adsorbents require additional pre-treatment in order to enhance their adsorption capacities and achieve the performance of activated carbons; therefore, several treatment methods have been investigated (Johari et al. 2016). The heat treatment is one of the best and simple methods of activation. However, calcination at high-temperature can affect the superficial functional groups and damages the pores structure, and loss of removal efficacy of chemicals by adsorbents after its thermal regeneration has been one of main limitation for wider use of different adsorbents including activated carbons (Wang and Zhu 2006).

In order to overcome this drawback, the objective of this present study was to find, whether thermal treatment of diatomite reduces the adsorption capacities of textile dye and enhances the selectivity and regenerability of the recycled materials in aqueous systems. To determine different parameters affecting the characteristics of regenerated diatomite using heat treatment, batch experiments were done in laboratory scale in normal conditions of temperature and pressure.

Materials and methods

Samples preparation

Diatomite used in this work was provided by the National Company for Non-ferrous Mining Products (ENOF), from Sig deposit, Mascara (West Algeria). After collection, the diatomite was dried at 105 °C until constant mass changes, and then gently crushed and sieved to 250 µm. Thermal treatment in three different temperatures was applied at 300, 600 and 900 °C for 2 h in a programmable muffle furnace, with a heating rate of 3 °C min^{-1}. Obtained materials are named RD (raw diatomite), DH300, DH600 and DH900 and stored in a glass bottle for further use without any additional treatment.

Characterization of adsorbents

The properties of the raw and heated diatomite were determined using various techniques. The particle size distribution was determined from wet dispersion using ultrasound with laser scattering particle size analyzer (Analysette 22 NanoTec, Fritsch, Germany). For particle size calculations Mie theory was used. The procedure consists to add a dry sample into the analyzer cell (filled with distilled water) until the laser beam obstruction was 5–7%. The different crystalline phases were determined using X-ray powder diffractometer (XRD), PANalytical X'Pert PRO MPD diffractometer equipped with an X'Celerator linear detector, using Cu-Kα_1 radiation (λ = 1.5406 Å), 40 kV voltages and 30 mA current. The diffraction patterns were recorded between 5 and 80° (2θ) with an angular step interval of 0.0334° and scanning speed of 1°/min. The surface morphology and chemical composition were obtained by field emission scanning electron microscopy (SEM, Tescan Mira/LMU) coupled with X-ray energy-dispersive spectrometry (EDX, Inca Energy 350). The specific surface area of each material was determined at liquid-nitrogen temperature (77 K) using the Brunauer, Emmett and Teller (BET) gas adsorption method using Quadrasorb SI-KR/MP (Quantachrome Instruments, Boynton Beach, FL). The samples were degassed at 100 °C for 24 h under vacuum prior to measurement. The total pore volumes were calculated based on N_2 adsorption–desorption,

while the pore-size distributions were calculated from the adsorption branch of the isotherm, according to the Barrett–Joyner–Halenda (BJH) model.

Batch adsorption experiments of Red ETL dye

An industrial textile dye appointed Red ETL (R-ETL) was used in this study as target pollution. The dye was provided by SOITEX wet-process textile industry of Tlemcen (West Algeria).

The removal study of R-ETL dye by RD, DH300, DH600 and DH900 consists to optimize on batch mode the physicochemical parameters affecting the adsorption process of R-ETL molecules onto the surface of adsorbents.

Batch experiments were carried out on a magnetic stirrer (Thermo Scientific Cimarec i Multipoint) at 400 rpm using 100 mL Erlenmeyer flask. A desired amount of adsorbent was added to 50 mL of R-ETL dye solution at known initial concentration; the mixture was stirred for desired contact time to ensure equilibrium. Then, the Erlenmeyer's content was centrifuged at 6500 rpm during 10 min, and the remaining concentration of R-ETL dye in solution was measured by analyzing the supernatant using UV–visible spectrophotometer (HACH DR 4000) at 508 nm wavelength. The adsorbed quantity (Q_e) of R-ETL dye adsorbed was calculated according to the following equation:

$$Q_e\left(\text{mg g}^{-1}\right) = \frac{(C_i - C_e)\cdot V}{W} \quad (1)$$

where C_i and C_e are, respectively, the initial and equilibrium concentration of R-ETL in solution (mg L^{-1}), V is the volume of solution (L), and W is the amount of adsorbents (g).

In order to determine the effective adsorption conditions, a set of experiments were performed with different pH values, contact time, adsorbents dose (solid/liquid ratio) and initial dye concentrations. The pH value of solution is an important parameter and especially in the adsorption studies of textile dyes, because it can affect not only the adsorption capacity, but also the behavior and solubility of dye molecules in water. The effect of this parameter was studied over the pH range from 2 to 10. The required pH value of solution was adjusted with diluted solutions of HNO_3 (0.1 N) and NaOH (0.1 N). The determination of equilibrium state between the liquid and solids phases was studied at different interval time from 5 to 180 min with an initial dye concentration of 50 mg L^{-1} and optimum pH value. The adsorbent dose can also be very useful for predicting the cost of material per unit of the effluent of dye solution to be treated. Under optimum conditions of pH and contact time, the effect of the ratio solid/liquid was examined from 0.5 to 10 g L^{-1}. Finally, the influence of the initial concentration of R-ETL dye onto the adsorption phenomena was studied at different initial concentrations ranging from 10 to 1000 mg L^{-1}, at optimized above cited parameters.

Regeneration and reusability

The regeneration of adsorbents is important from an economical point of view; the adsorbents recycling is considered as an important aspect to minimize the costs related to the synthesis of materials. Under the optimum obtained conditions, the thermal treatment was used as regeneration method. 04 g of raw diatomite was mixed with 1 L of R-ETL dye solution at 1 g L^{-1} until the saturation. Then, the thermal regeneration was performed at 300, 600 and 900 °C during 2 h. Ethanol and deionized water were used as eluent to check the remaining amount of R-ETL after heat treatment. Moreover, in order to evaluate the reusability of regenerated materials, three loading cycles were carried out. The percentage adsorption of dye was obtained using the following equation:

$$R\,(\%) = \frac{(C_i - C_e)}{C_i} \times 100 \quad (2)$$

Adsorption kinetics

The modeling of kinetics studies allows to describe the mechanisms and phenomena that control the adsorption process using theoretical models. The adsorption kinetics of R-ETL dye on RD, DH300, DH600 and DH900 have been tested on many theoretical models reported in the literature (see Table 1).

Table 1 Lists of kinetic adsorption models and their linearized expressions

Kinetic models	Nonlinear form	Linear equation	References
Pseudo-first order	$Q_t = Q_e[1 - \exp(-k_{1p}t)]$	$\ln(Q_e - Q_t) = \ln Q_e - k_{1p}t$	Lagergren (1898)
Pseudo-second order	$Q_t = k_{2p}Q_e^2 t/(1 + Q_e k_{2p}t)$	$t/Q_t = 1/k_{2p}Q_t^2 + t/Q_e$	Ho and McKay (1999)
Intra-particle diffusion	$Q_t = k_p t^{0.5}$	$Q_t = k_p t^{0.5}$	Weber and Morris (1963)
Extra-particle diffusion	$F(t) = \frac{C_0 - C_t}{C_0 - C_e} = \frac{Q_t}{Q_e} = \left[1 - \exp\left(-\frac{\pi^2 D}{r^2}t\right)\right]^{\frac{1}{2}}$	$\ln\left[1 - F(t)^2\right] = \frac{\pi^2 D}{r^2}t$	Al-Ghouti et al. (2005)

Table 2 Lists of adsorption isotherm models and their linearized expressions

Isotherms	Nonlinear form	Linear equation	References
Freundlich	$Q_e = K_F (C_e)^{1/n}$	$\ln Q_e = \ln K_F + n^{-1} \ln C_e$	Freundlich (1906)
Langmuir	$Q_e = (Q_{max} K_L C_e)/(1 + K_L C_e)$	$C_e/Q_e = (1/K_L Q_{max}) + (C_e/Q_{max})$	Langmuir (1917)
Dubinin–Radushkevich	$Q_e = Q_{max} \exp(-D_{DR} \varepsilon^2)$ $\varepsilon = RT \ln (1 + C_e^{-1})$	$\ln Q_e = \ln Q_{max} - K_{ad} \varepsilon^2$ $\varepsilon = RT \ln (1 + C_e^{-1})$	Dubinin and Radushkevich (1947)
BET	$Q_e = \frac{Q_s C_{BET} C_e}{(C_s - C_e)[1+(C_{BET}-1)(C_e/C_s)]}$	$\frac{C_e}{Q_e(C_s-C_e)} = \frac{1}{Q_s C_{BET}} + \frac{(C_{BET}-1)}{Q_s C_{BET}} \frac{C_e}{C_s}$	Ebadi et al. (2009)

Adsorption isotherm

The modeling of adsorption isotherms is to describe in a wide range of concentration and temperature, experimental results with mathematical equations. Several isotherm models have been proposed for the adsorption study, and the main models are described in Table 2.

Error calculation

In recent decades, the linear regression has been one of the most viable tools used to define the best-fitting relationship and the correlation coefficient was the only indicator confirming the consistency of the theoretical assumptions of the kinetic and isotherm adsorption models (Foo and Hameed 2010). To check the validity of the above-mentioned models, the standard statistics of root-mean-squared error (RMSE) was calculated (Eq. 3) in addition to the correlation coefficient to support the best fit adsorption model.

$$\mathrm{RMSE} = 100\sqrt{\frac{1}{N}\sum_{i-1}^{N}\left(q_t^{\exp} - q_t^{\mathrm{cal}}\right)_i^2} \quad (3)$$

where $q_t^{\exp}$ and q_t^{cal} (mg g^{-1}) are, respectively, the observed and predicted amounts of R-ETL dye adsorbed, and N is the number of experiments.

Results and discussion

Characterizations

Table 3 summarizes the chemical composition and the physical properties of raw and heated diatomite.

It shows that the main elements for all materials are: O, C, Si, Ca and Al together with other mineral impurities as Fe, Mg, K, Na, etc. The high contents of Si, Ca, O and C correspond, respectively, to the silica frustules of diatoms and carbonate minerals, while the Al content indicates the presence of aluminosilicate minerals (Sun et al. 2013). The decrease in O and C during the heat treatment indicates the elimination of organic matter, while the increase of other elements designates purification and phase transformation of heated materials.

Table 3 The chemical compositions of thermal treated diatomite

Elemental composition (%)	RD	DH300	DH600	DH900
O	58.12	44.84	35.67	32.10
C	8.58	12.67	5.60	1.60
Si	30.38	39.43	41.00	43.87
Ca	4.60	2.9	3.8	4.20
Al	0.93	0.78	1.98	2.73
Fe	0.27	0.19	0.94	1.13
Mg	0.42	0.17	0.47	0.98
K	0.08	0.11	0.61	0.71
Na	0.78	0.23	0.39	0.26
Ignition loss (%)	–	0.00	0.39	0.49

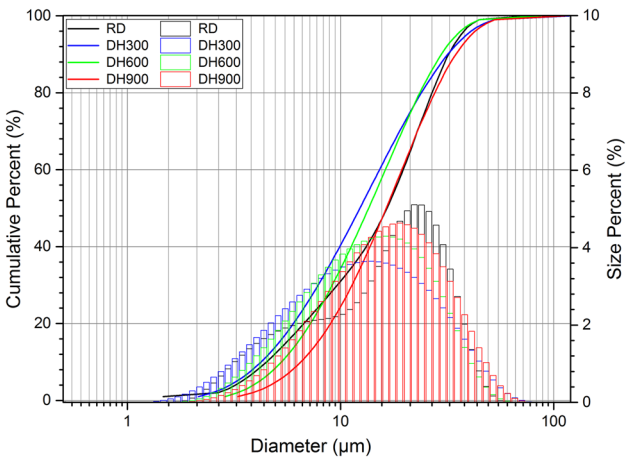

Fig. 1 Dynamic light-scattering size distribution of RD, DH300, DH600 and DH900 in the aqueous suspensions

Particle size and pore distribution analysis (Fig. 1) shows that the coefficients of uniformity (C_u = D60/D10) are more then 2 (4.39; 3.60; 3.07; 2.98, respectively, for RD, DH300, DH600 and DH900) indicating a spread granulometry of all materials. As the value of C_u decreases (close to 2) by increasing temperature, it means that the distribution of

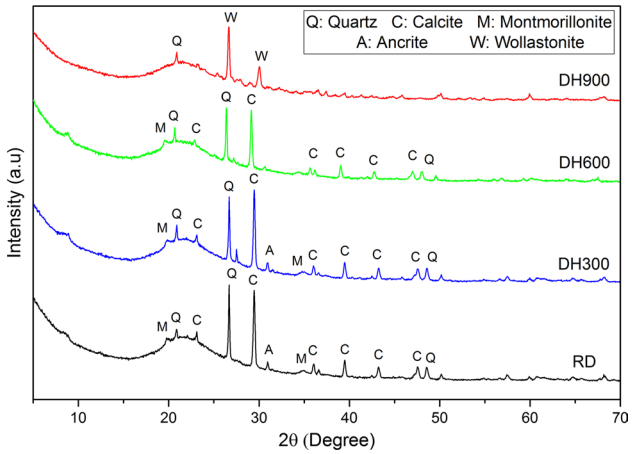

Fig. 2 XRD patterns of RD, DH300, DH600 and DH900

particle becomes more uniform due to the elimination of impurities.

X-ray patterns obtained from raw and heated diatomite are shown in Fig. 2. The broad diffraction at approximately 22° of 2θ is characteristic of non-crystalline opal-A, which could be identified as biogenic hydrated amorphous silica (Sun et al. 2013). Some mineral impurities as montmorillonite and ancrite are also found in the diatomite samples. After thermal treatment, the mineral structure of diatomite was not dramatically changed up to 600 °C, except a slight decrease in the pattern intensity of Calcite and Quartz. However, a new crystalline phase wollastonite appears on the XRD pattern of DH900. The appurtenance of wollastonite patterns can be explained by the reaction between the lime liberated from the decomposition of calcite and silica of diatoms skeletons which is found in abundance (Ibrahim and Selim 2012); this reaction is also followed by the desperation of calcite and quarts patterns.

As seen in Fig. 3, the SEM micrographs (b) and (c) still show the original form of diatoms genus *Coscinodiscus Ehrenberg* (Centrales). The disc-shaped diatomite treated at 600 °C has highly developed porous network

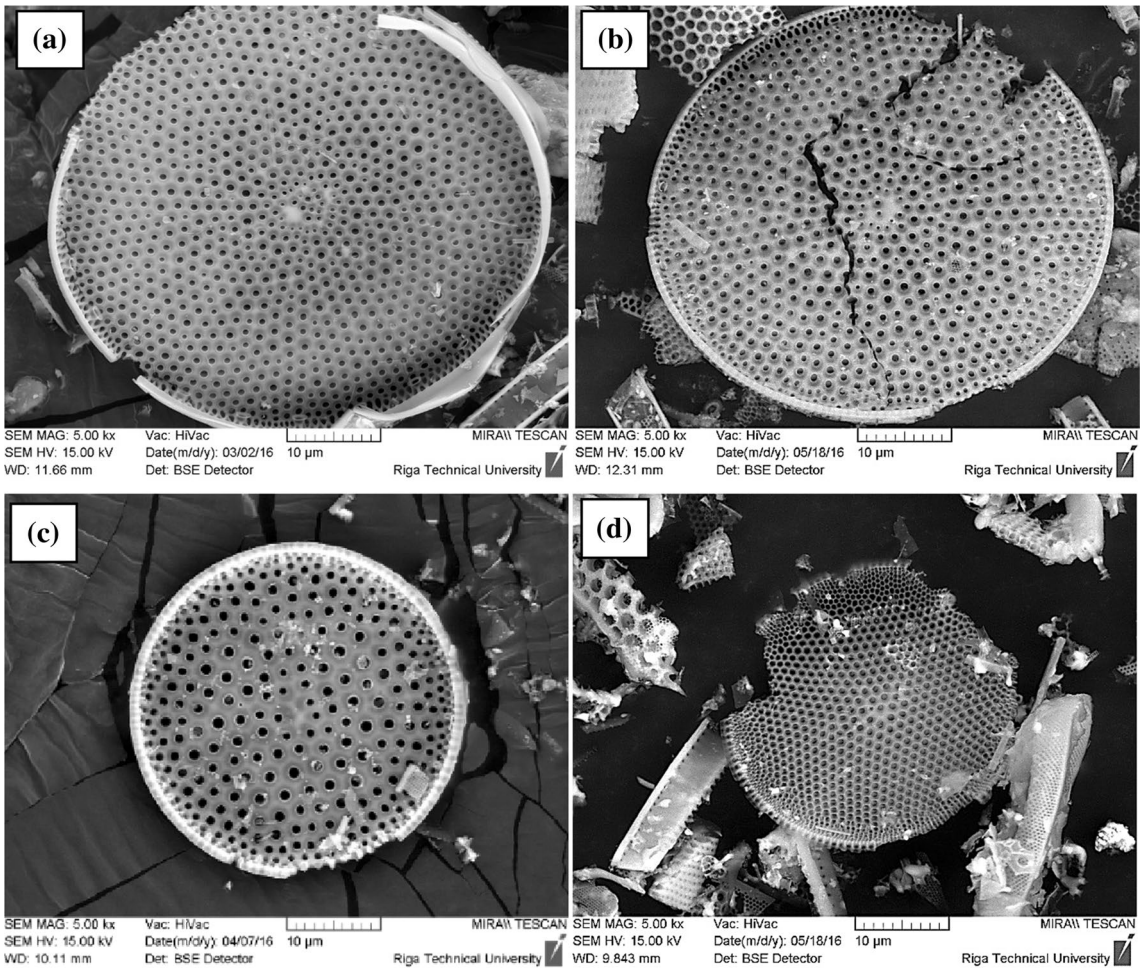

Fig. 3 Scanning electron micrograph of heated diatomite **a** RD, **b** DH300 **c** DH600 and **d** DH900

ranging between macroporous and mesoporous structure. In addition, the concave and convex aspects of the surface were almost disappeared and smoother surface was formed due to the removal of impurities and organic matter. As reported by Ediz et al. (2010) that the heat treatment is the suitable method to increase the permeability of diatomite. The deconstruction of the shape and pores collapsing of diatom skeleton were occurred at 900 °C. The same finding was reported by Rangsriwatananon et al. (2008), regarding the form of diatoms at different thermal and acid treatments.

Nitrogen adsorption/desorption isotherms (inset in Fig. 4) and corresponding Barrett, Joyner and Halenda (BJH) pore-size distribution curves of RD, DH300, DH600 and DH900 samples are shown in Fig. 4. The N_2 adsorption/desorption diatomites exhibit type II adsorption isotherms with H3 hysteresis loop according to the International Union of Pure and Applied Chemistry (IUPAC) classification (Gregg and Sing 1982). The hysteresis loop of this isotherm is associated with the filling and emptying of the mesopores by capillary condensation, implying that the pores are mainly narrow and slit-like (Sing and Williams 2004). In addition, increasing in the sharp of N_2 adsorbed quantity near the relative pressure of 1 reflecting the existence of macropores in all samples, except DH900 sample.

The textural parameters of the raw and heated diatomite samples such as the specific surface area (S_{BET}), pore volume (V_{pore}) and average pore size (W) are summarized in Table 4.

It evident to say that up to 600 °C the isotherms shape of the heated samples was not greatly affected, and the average pore size was improved due to the elimination of natural organic impurities. However, the treatment of diatomite at higher temperatures (900 °C) decreases not only the nitrogen adsorption, which is indicated by a weakening of the hysteresis, but also the specific surface area and pores volume. The average pore size was slightly decreased reflecting the deconstruction of the porous structure of diatoms frustule.

Table 4 Textural parameters of the heated diatomite samples at different temperatures

Samples	Specific surface area S_{BET} ($m^2\ g^{-1}$)	Pore volume V_{pore} ($cm^3\ g^{-1}$)	Average pore size W (nm)
RD	31.65	0.046	3.79
D300	27.88	0.041	3.82
D600	20.54	0.035	4.00
D900	5.17	0.009	3.96

Adsorption of R-ETL dye

Effect of pH solution

As shown in Fig. 5, the pH of solution affects significantly the adsorption of R-ETL dye. A decrease in the adsorption capacity with increasing pH medium was noted. The maximum quantities of R-ETL adsorbed were obtained at pH 2 with 12.7, 13.5, 15.2 and 8.8 mg g^{-1}, respectively, for RD, DH300, DH600 and DH900, while the lowest quantities were recorded at pH 10 with 0.43, 0.1, 2.3 and 1.2 mg g^{-1} for RD, DH300, DH600 and DH900, respectively.

The highest adsorption capacities obtained at acidic condition might be due to the protonation effect of superficial functional groups of adsorbents, providing a strong electrostatic attractive forces between the surface of adsorbents and the negatively charged R-ETL dye molecules. The lower adsorption capacities observed at alkaline

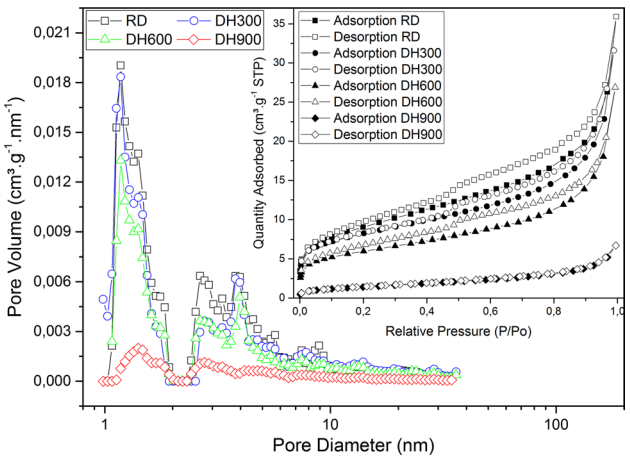

Fig. 4 Particle size distributions curves and nitrogen, adsorption–desorption isotherms (the inset) of heated diatomite samples

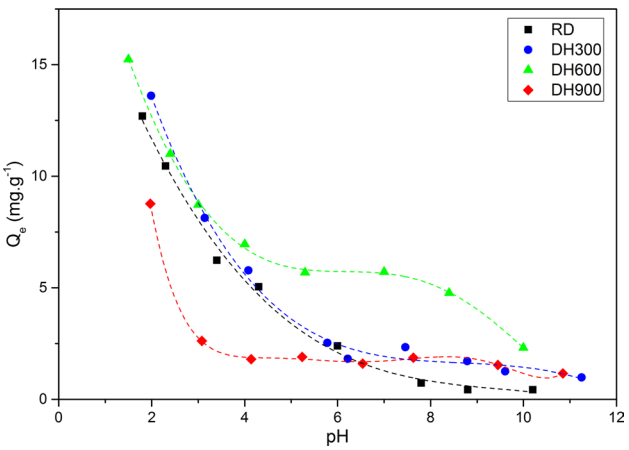

Fig. 5 Influence of pH solution on the adsorption capacity of R-ETL dye onto RD, DH300, DH600 and DH900

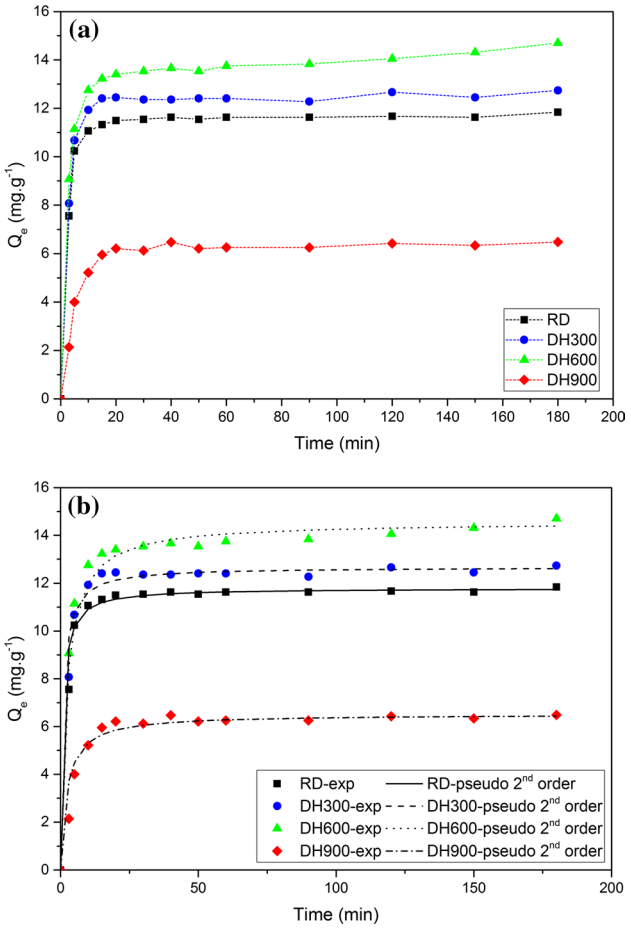

Fig. 6 **a** Effect of contact time on the adsorption process of R-ELT dye; **b** kinetic adsorption using pseudo-second-order model for modeling the adsorption of R-ETL dye onto RD, DH300, DH600 and DH900

condition are probably due to the competition between the excess hydroxyl ions and the negative R-ETL dye molecules to occupy the same binding sites (Ncibi et al. 2009).

Effect of contact time

The results illustrated in Fig. 6a show a rapid increase in adsorption capacity during the first 20 min, where an adsorption amount of 11.3, 12.5, 13, 5 and 6.2 mg g^{-1} was recorded, respectively, for RD, DH300, DH600 and DH900. The time required to reach equilibrium between RD, DH300, DH600 and DH900 and the R-ETL dye solution is 30 min. The extension of the contact time up to 180 min (3 h) leads to an insignificant improvement, and the adsorption capacity remains almost constant.

The rapid increase in the adsorbed quantity at the initial stage is probably due to the abundance of active sites easily accessible by the R-ETL dye molecules. The slowdown of the adsorption rate may be due either to the reduced of the available active sites on the surface or to the saturation stat of the adsorbents, which causes repulsive forces between the adsorbed dye molecules onto the surface and the remaining dye molecules in the solution (El Haddad et al. 2012).

The kinetic study of R-ETL dye onto RD, DH300, DH600 and DH900 is important to understand the dynamics of the adsorption reaction in terms of order of the rate constant. Thus, the kinetics parameters provide information for designing and modeling of the adsorption process. Four kinetic models: pseudo-first order, pseudo-second order, intra-particle diffusion and extra-particle diffusion were used to examine the experimental data.

Apart from the correlation coefficient (R^2), RMSE was used to measure the goodness-of-fit. Table 5 regroups the values of kinetic parameters, correlation coefficients (R^2), and the calculated errors for each model.

Except the pseudo-second-order kinetic model, the low correlation coefficients and the high RMSE errors confirm that the other kinetic models do not give a good regression, indicating a poor description of the removal phenomena of R-ETL molecules by RD, DH300, DH600 and DH900.

Table 5 Kinetic parameters for the adsorption of R-ETL dye onto RD, DH300, DH600 and DH900

	Pseudo-first order					Pseudo-second order				
	Q_e^{exp}	Q_e^{cal}	k_{1p}	RMSE	R^2	Q_e^{exp}	Q_e^{cal}	k_{2p}	RMSE	R^2
RD	11.84	0.97	0.0096	3.06	0.19	11.84	11.79	0.11	0.48	0.99
DH300	12.74	1.08	0.0098	3.29	0.19	12.74	12.67	0.09	0.49	0.99
DH600	14.70	2.77	0.0110	3.33	0.48	14.70	14.56	0.03	0.44	0.99
DH900	6.482	0.78	0.0112	1.88	0.14	6.482	6.51	0.07	0.47	0.99

	Intra-particle diffusion			Extra-particle diffusion		
	k_p	RMSE	R^2	D (cm^2 s^{-1})	RMSE	R^2
RD	0.47	2.44	0.37	1.05E−06	3.00	0.47
DH300	0.51	2.62	0.37	1.05E−06	3.23	0.43
DH600	0.62	2.71	0.45	8.87E−07	3.27	0.69
DH900	0.34	1.32	0.52	1.31E−06	1.69	0.64

However, the best correlations were obtained for the pseudo-second-order kinetic model with highest R^2 (0.99) and lowest RMSE errors. Furthermore, the calculated Q_e values through this model are close to the experimental values (see Fig. 6b). This strongly suggests that the adsorption of R-ETL molecules onto raw and heated diatomite is most appropriately represented by the pseudo-second-order kinetic model, supposing that two reactions either in series or in parallel are occurring, the first one is fast and reaches equilibrium quickly and the second is a slower reaction that can continue for a long period of time.

Effect of adsorbent dosage

Figure 7 depicts the effect of adsorbents dosage on the adsorption capacity of R-ETL dye. As shown in Fig. 8, the increase in the adsorbent dosage leads to the increase in the adsorption capacity. For instance, by increasing the adsorbents concentration from 0.5 to 10 g L^{-1} the adsorption increased from 0.97 to 5.33; 1.24 to 5.84; 1.63 to 8.57; 0.88 to 3.00, respectively, for RD, DH300, DH600 and DH900. This fact is mainly due to a substantial increase in the number of active sites available on the surface of the tested adsorbents. Further, by increasing the adsorbent concentration up to 10 g L^{-1} the adsorbed amount remains constant. This may due to the saturation of the available active sites or to the equilibrium stat established between the adsorbed dye molecules and those remain in the solution at the studied initial dye concentration (Ncibi et al. 2009).

Effect of initial dye concentration

It can be seen from Fig. 8a that at lower concentration values ($C_0 < 200$ mg L^{-1}) the uptake capacity increased from 0.19 to 34.86; 2.68 to 52.23; 3.3 to 51.64 and 0.1 to 39.38 mg g^{-1},

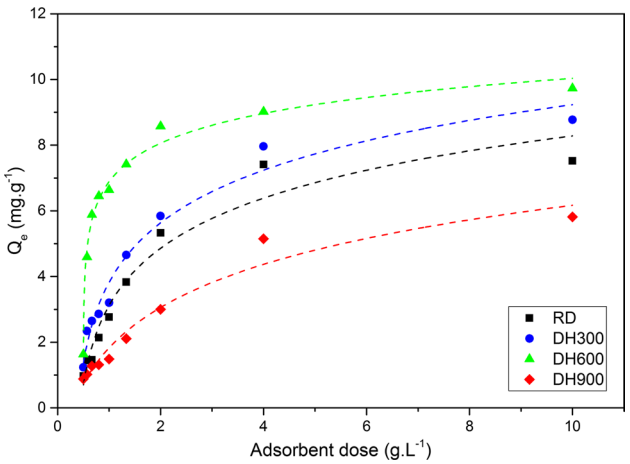

Fig. 7 Effect of adsorbent dosage on the adsorption capacities of R-ETL dye onto RD, DH300, DH600 and DH900

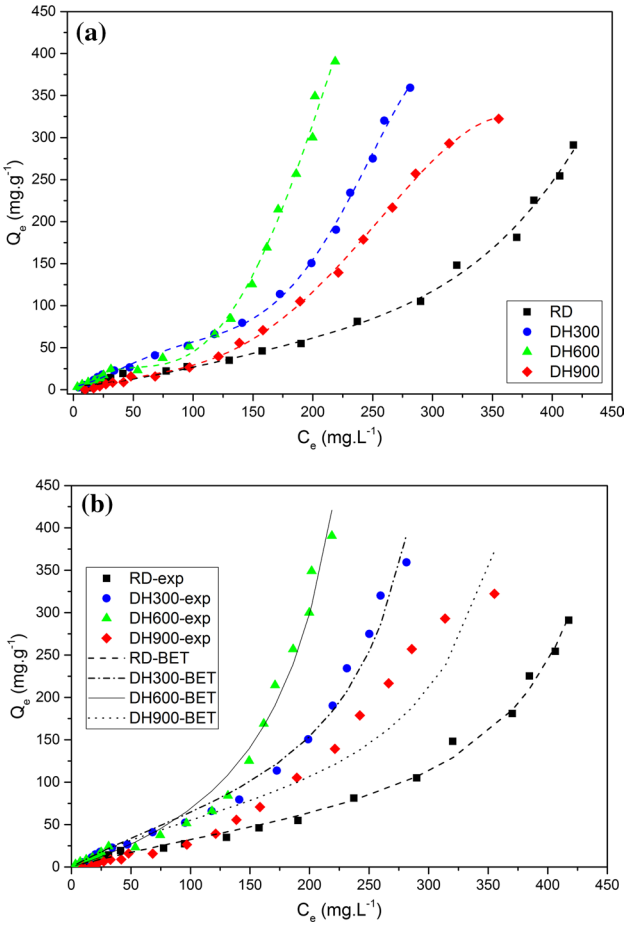

Fig. 8 **a** Influence of the initial R-ETL dye concentration onto the adsorption process; **b** adsorption isotherm using BET model for modeling the adsorption of R-ETL dye onto RD, DH300, DH600 and DH900

respectively, for RD, DH300, DH600 and DH900 as the initial dye concentration increased from 10 to 200 mg L^{-1}. Afterward, by further increasing the R-ETL dye concentration (up to 1000 mg L^{-1}) the adsorption behavior of R-ETL dye displays a point of inflexion and the adsorption capacities reach 291.15; 359.29; 390.64 and 322.36 mg g^{-1}, respectively, for RD, DH300, DH600 and DH900. This same phenomenological was reported by Bisinella Scheufele (Bisinella et al. 2016) for the adsorption of RB5G dye on sugarcane bagasse.

This effect could be explained as: (1) At lower initial dye concentrations, all R-ETL dye molecules could interact with the binding sites on the adsorbents surface and high sorption rates occur which lead to the formation of monolayer (one molecule is adsorbed per site). After that, the binding sites on the adsorbents surface became saturated and no further adsorption occurs; (2) At high initial R-ETL dye concentrations the driving force increases due to the gradient of concentration at solid/liquid interface generating a strong

adsorbate–adsorbate interaction, which promote the formation of other layers (multilayer adsorption) involving some intermolecular interactions (as van der Waals forces) supplemented by various electrostatic contributions (as polarization, field–dipole and field gradient–quadrupole interactions) between the molecules of R-ETL dye (Naderi 2014).

In order to better understand the mechanisms involved in the adsorption process of R-ETL dye onto RD, DH300, DH600 and DH900, it is important to establish a more appropriate relationship between the adsorption capacity (Q_e) and the equilibrium concentration (C_e). Various adsorption isotherm models: Freundlich, Langmuir, Dubinin–Radushkevich and BET were employed. The calculated isotherm constants and error values obtained for each model are given in Table 6.

The negative obtained values of Langmuir constants (Q_{max} and K_L) describe that the adsorption process of R-ETL dye did not follow Langmuir isotherm model, since K_L indicate the adsorption binding energy on the surface. Furthermore, and except the isotherm data of DH900 which is best-fitted by Freundlich isotherm model with a correlation coefficient of 0.94 and RMSE of 11.58, the BET isotherm model is the most appropriate to describe the adsorption of R-ETL dye on RD, DH300 and DH600 (see Fig. 8b) with a correlation coefficient of 0.99, 0.98, 0.98, respectively. These best correlations confirming the assumptions of mono- and multi-layers phenomenological involved during the adsorption process of R-ETL onto the surface of adsorbents.

Effect of calcination temperature on the adsorption capacity

The structure of diatomite from the one hand was affected by the calcination process but form the other hand the adsorption capacities were improved. Based on the chemical compositions, the RD show some natural organic impurities sticks on the surface which may intervene in the adsorption of N_2 gas and give more surface area than the heated samples. These organics matter probably competes the molecule of R-ETL dye to be absorbed into the surface. After calcination, at 300 °C the adsorption capacity improved due to transformation of this organic matter to coal (12.67%). Afterward, the heating up at 600 °C burn out all the organic impurities from the pores and makes the surface smoother (see Fig. 3c) which facilitate the interaction between the R-ETL dye molecules and the functional groups onto the surface of adsorbent that explain the highest adsorption quantity of dye on DH600. The calcination at 900 °C is not suitable as method of treatment, because the most structural characteristics including the surface area of diatoms frustule were damaged.

Material recycling

Figure 9a, b shows, respectively, the number of adsorption reusability cycles and UV–visible absorption spectrum of the released amount of R-ETL dye after thermal regeneration. It is clear that the recovery of R-ETL dye from aqueous solution slightly decreases and around 10% of removal efficiency was lost after each regeneration cycle. The recycled samples can restore up to 66.4, 73.35 and 67.85%, respectively, for DH300, DH 600 and DH900 after three thermal regeneration cycles. Even, the absorbance of the released amount was decreased in both UV and Visible ranges with increasing of thermal regeneration. As well illustrated in Fig. 9b, during thermal regeneration the organic dye substances adsorbed onto the surface or in pores decomposes to carbon. Thereafter, by increasing temperature up to 600 °C, the carbon formed oxidizes in air and disappears completely from the surface, making

Table 6 Adsorption isotherm constants for the adsorption of R-ETL dye onto RD, DH300, DH600 and DH900

	Freundlich				Langmuir			
	$1/n$	K_F	RMSE	R^2	K_L	Q_{max}	RMSE	R^2
RD	1.39	51.82	21.22	0.90	− 2.18E−03	− 89.70	53.10	0.66
DH300	1.12	432.62	40.31	0.98	− 2.18E−03	− 241.58	42.90	0.86
DH600	1.13	493.71	64.30	0.93	− 8.00E−04	− 143.93	48.25	0.85
DH900	1.85	7.24	11.58	0.94	− 2.80E−03	− 66.70	27.58	0.93
	BET					Dubinin–Radushkevich		
	C_{BET}	Q_m	C_s	RMSE	R^2	Q_{max}	K_{ad}	RMSE	R^2
RD	3.67	54.88	506.55	6.77	0.99	91.02	1.00E−04	86.78	0.75
DH300	3.40	79.49	347.47	14.25	0.98	67.19	2.00E−05	115.54	0.42
DH600	1.01	125.39	284.01	16.63	0.98	65.07	9.00E−06	131.37	0.32
DH900	4.99	70.80	434.28	31.65	0.92	61.80	1.00E−04	105.87	0.71

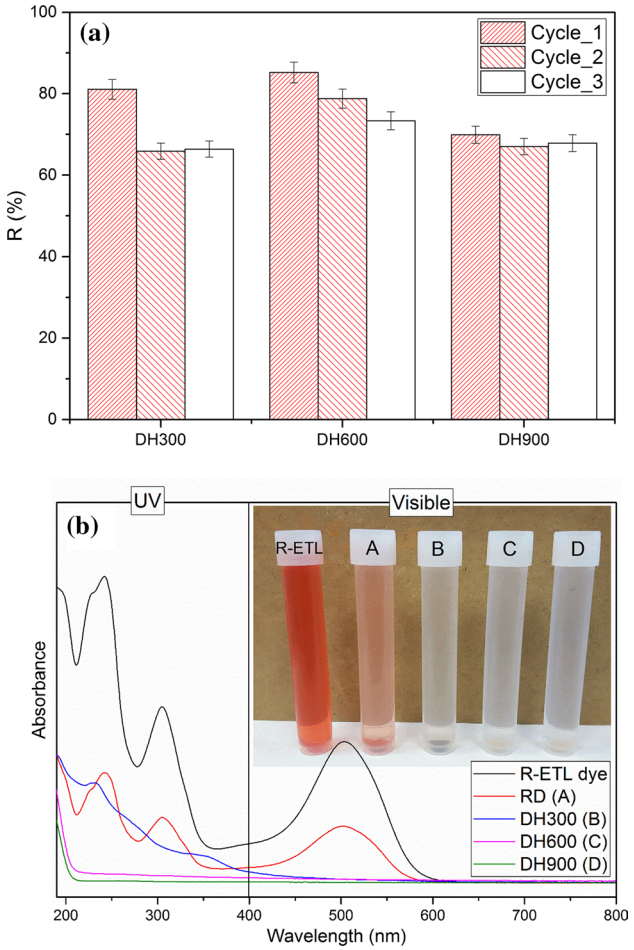

Fig. 9 **a** Reusability cycles of regenerated samples to remove R-ETL dye; **b** UV–visible absorption spectra of R-ETL dye obtained from different samples after thermal regeneration

the pores free and fresh for further adsorption cycles (Vimonses et al. 2009b).

Conclusion

In this study, the heat treatment of diatomite was used for the one hand to improve its adsorption capacities for textile dye removal, and for the other hand as regeneration approach in water purification field. We showed that the specific surface area and pore volume are the main affected textural characteristics, but the macro-structure pores network of heated diatomites remains intact after calcination. At low temperatures (less than 600 °C), the mineral phases remain unchangeable, and the disk shape of treated samples still shows the original form of diatoms skeletons. The maximum adsorption capacities were obtained at low pH value (pH 2), and high adsorbent dose (4 g L^{-1}). Based on the effect of contact time, the adsorption process was fast and the equilibrium was rather short which reached after 30 min. The kinetic studies were well represented by the pseudo-second-order kinetic model. The isotherm adsorption revealed that the BET model describes satisfactorily the adsorption process of R-ETL dye onto RD, DH300 and DH600, while Freundlich model is more appropriate to the adsorption of R-ETL onto DH900. The mono- and multilayer adsorption phenomenological of R-ETL dye is the main assumptions for the present adsorption process. Our findings allow to conclude that the thermal treatment is an effective method of treatment which lead to enhance the adsorption capacities of diatomite and promote the possibilities for material recovery and recycling.

Acknowledgements The authors gratefully acknowledge the financial support provided by the Algerian Ministry of Superior Education and Scientific Research (PNE Program No. 682, Code 16/70682). The authors would like to acknowledge the assistance provided by Mr Kristaps Rubenis, Ms Inga Dušenkova and Ms Valentīna Stepanova, from Rudolfs Cimdins Riga Biomaterials Innovations and Development Center, Institute of General Chemical Engineering, Faculty of Materials Science and Applied Chemistry, Riga Technical University, Latvia, respectively, for SEM micrographs, laser scattering particle size analyzes and BET analyzes. In the end the authors would like to dedicate this work for Prof. Ouali Mohand Said, from Abdelhamid Ibn Badis University, Mostaganem (Algeria), may he rest in peace.

List of symbols

C_i	Initial concentration of R-ETL dye (mg L^{-1})
C_e	Equilibrium concentration of R-ETL dye (mg L^{-1})
Q_e	Adsorbed quantity of R-ETL dye (mg g^{-1})
V	Volume of solution (L)
W	Amount of adsorbents (g)
R	Removal efficiency of R-ETL dye (%)
t	Time (min)
Q_t	Amount of R-ETL dye adsorbed at time t (mg g^{-1})
k_{1p}	Pseudo-first-order kinetic model constant (min^{-1})
k_{2p}	Pseudo-second-order kinetic model constant (g mg^{-1} h^{-1})
k_p	Intra-particle diffusion kinetic model constant (g mg^{-1} $min^{-0.5}$)
C_t	Concentration at time t (mg L^{-1})
D	Intra-particle diffusion coefficient (m^2 s^{-1})
r	Particle radius assuming spherical geometry (m)
K_F	Freundlich constant (mg g^{-1}) (L g^{-1})$^{1/n}$
$1/n$	Freundlich exponent
K_L	Langmuir isotherm constant (L mg^{-1})
Q_{max}	Maximum adsorption capacity of R-ETL dye (mg g^{-1})
D_{DR}	Dubinin–Radushkevich isotherm constant (mol^2 kJ^{-2})
T	Temperature (K)
R	Ideal gas constant (J K^{-1} mol^{-1})

C_{BET}	BET adsorption isotherm constant (L/mg)
C_s	Saturation concentration of R-ETL dye (mg L^{-1})
Q_s	Monolayer adsorption capacity (mg g^{-1})
RMES	Root-mean-squared error
q_e^{exp}	Observed amounts of R-ETL dye adsorbed (mg g^{-1})
q_e^{cal}	Predicted amounts of R-ETL dye adsorbed (mg g^{-1})
N	Number of experimental measurements
C_u	Coefficients of uniformity
D10	Intercepts for 10% of the cumulative mass
D60	Intercepts for 60% of the cumulative mass

References

Abidi N, Errais E, Duplay J et al (2015) Treatment of dye-containing effluent by natural clay. J Clean Prod 86:432–440. https://doi.org/10.1016/j.jclepro.2014.08.043

Akar ST, Özcan AS, Akar T et al (2009) Biosorption of a reactive textile dye from aqueous solutions utilizing an agro-waste. Desalination 249:757–761. https://doi.org/10.1016/j.desal.2008.09.012

Al-Ghouti M, Khraisheh MAM, Ahmad MNM, Allen S (2005) Thermodynamic behaviour and the effect of temperature on the removal of dyes from aqueous solution using modified diatomite: A kinetic study. J Colloid Interface Sci 287:6–13. https://doi.org/10.1016/j.jcis.2005.02.002

Aziz A, Ouali MS, Elandaloussi EH et al (2009) Chemically modified olive stone: a low-cost sorbent for heavy metals and basic dyes removal from aqueous solutions. J Hazard Mater 163:441–447. https://doi.org/10.1016/j.jhazmat.2008.06.117

Belala Z, Jeguirim M, Belhachemi M et al (2011) Biosorption of basic dye from aqueous solutions by Date Stones and Palm-Trees Waste: kinetic, equilibrium and thermodynamic studies. DES 271:80–87. https://doi.org/10.1016/j.desal.2010.12.009

Bhatti HN, Nausheen S (2014) Equilibrium and kinetic modeling for the removal of Turquoise Blue PG dye from aqueous solution by a low-cost agro waste. Desalin Water Treat. https://doi.org/10.1080/19443994.2014.927799

Bisinella F, Nivaldo A, Eduardo C et al (2016) Monolayer–multilayer adsorption phenomenological model: kinetics, equilibrium and thermodynamics. Chem Eng J 284:1328–1341. https://doi.org/10.1016/j.cej.2015.09.085

Chen J, Pan X, Chen J (2013) Regeneration of activated carbon saturated with odors by non-thermal plasma. Chemosphere 92:725–730. https://doi.org/10.1016/j.chemosphere.2013.04.014

de Sales PF, Magriotis ZM, de LS Rossi MA et al (2013) Study of chemical and thermal treatment of kaolinite and its influence on the removal of contaminants from mining effluents. J Environ Manag 128:480–488. https://doi.org/10.1016/j.jenvman.2013.05.035

Devi S, Murugappan A, Rajesh Kannan R (2015) Sorption of reactive blue 19 onto freshwater algae and seaweed. Desalin Water Treat 54:2611–2624. https://doi.org/10.1080/19443994.2014.902333

Djafer A, Kouadri Moustefai S, Iddou A, Si Ali B (2014) Study of bimacid dye removal from aqueous solution: a comparative study between adsorption on pozzolana, bentonite, and biosorption on immobilized anaerobic sulfate-reducer cells. Desalin Water Treat 52:7723–7732. https://doi.org/10.1080/19443994.2013.833866

Djilani C, Zaghdoudi R, Djazi F et al (2015) Adsorption of dyes on activated carbon prepared from apricot stones and commercial activated carbon. J Taiwan Inst Chem Eng 53:112–121. https://doi.org/10.1016/j.jtice.2015.02.025

Dubinin MM, Radushkevich LV (1947) The equation of the characteristic curve of the activated charcoal. Proc Acad Sci USSR Phys Chem Sect 55:331–337

Ebadi A, Soltan Mohammadzadeh JS, Khudiev A (2009) What is the correct form of BET isotherm for modeling liquid phase adsorption? Adsorption 15:65–73. https://doi.org/10.1007/s10450-009-9151-3

Ediz N, Bentli I, Tatar I (2010) Improvement in filtration characteristics of diatomite by calcination. Int J Miner Process 94:129–134. https://doi.org/10.1016/j.minpro.2010.02.004

El Haddad M, Mamouni R, Saffaj N, Lazar S (2012) Removal of a cationic dye—Basic Red 12—from aqueous solution by adsorption onto animal bone meal. J Assoc Arab Univ Basic Appl Sci 12:48–54. https://doi.org/10.1016/j.jaubas.2012.04.003

Foo KY, Hameed BH (2010) Insights into the modeling of adsorption isotherm systems. Chem Eng J 156:2–10. https://doi.org/10.1016/j.cej.2009.09.013

Freundlich HMF (1906) Over the adsorption in solution. J Phys Chem 57:385–471

Gregg SJ, Sing KSW (1982) Adsorption, surface area and porosity, 2nd edn. Academic Press, London

Ho YS, McKay G (1999) Pseudo-second order model for sorption processes. Process Biochem 34:451–465. https://doi.org/10.1016/S0032-9592(98)00112-5

Ibrahim SS, Selim AQ (2012) Heat treatment of natural diatomite. Physicochem Probl Miner Process 48:413–424. https://doi.org/10.5277/ppmp120208

Iddou A, Ouali MS (2008) Waste-activated sludge (WAS) as Cr(III) sorbent biosolid from wastewater effluent. Colloids Surf B Biointerfaces 66:240–245. https://doi.org/10.1016/j.colsurfb.2008.06.018

Iddou A, Hadj Youcef M, Aziz A, Ouali MS (2011) Biosorptive removal of lead (II) ions from aqueous solutions using *Cystoseira stricta* biomass: study of the surface modification effect. J Saudi Chem Soc 15:83–88. https://doi.org/10.1016/j.jscs.2010.10.007

Johari K, Saman N, Song ST et al (2016) Adsorption enhancement of elemental mercury by various surface modified coconut husk as eco-friendly low-cost adsorbents. Int Biodeterior Biodegrad 109:45–52. https://doi.org/10.1016/j.ibiod.2016.01.004

Kelewou H, Merzouki M, Lhassani A (2014) Biosorption of textile dyes Basic Yellow 2 (BY2) and Basic Green 4 (BG4) by the live yeast Saccharomyces cerevisiae. J Mater Environ Sci 5:633–640

Lagergren S (1898) Zur theorie der sogenannten adsorption geloster stoffe. K. Sven. Vetenskapsakademiens. Handl 24:1–39

Langmuir I (1917) The Constitution and Fundamental Properties of Solids and Liquids. J Am Chem Soc 39:1848–1906. https://doi.org/10.1021/ja02254a006

Mahmoodi NM, Arami M (2008) Modeling and sensitivity analysis of dyes adsorption onto natural adsorbent from colored textile wastewater. J Appl Polym Sci 109:4044–4048. https://doi.org/10.1002/app

Mahmoodi NM, Hayati B, Arami M, Lan C (2011) Adsorption of textile dyes on Pine Cone from colored wastewater: kinetic, equilibrium and thermodynamic studies. Desalination 268:117–125. https://doi.org/10.1016/j.desal.2010.10.007

Mittal A, Mittal J, Malviya A, Gupta VK (2009) Adsorptive removal of hazardous anionic dye "Congo red" from wastewater using waste materials and recovery by desorption. J Colloid Interface Sci 340:16–26. https://doi.org/10.1016/j.jcis.2009.08.019

Naderi M (2014) Surface area: Brunauer–Emmett–Teller (BET). Prog Filtr. https://doi.org/10.1016/b978-0-12-384746-1.00014-8

Ncibi MC, Mahjoub B, Ben Hamissa AM et al (2009) Biosorption of textile metal-complexed dye from aqueous medium using *Posidonia oceanica* (L.) leaf sheaths: mathematical modelling. Desalination 243:109–121. https://doi.org/10.1016/j.desal.2008.04.018

Rangsriwatananon K, Chaisena A, Thongkasam C (2008) Thermal and acid treatment on natural raw diatomite influencing in synthesis of sodium zeolites. J Porous Mater 15:499–505. https://doi.org/10.1007/s10934-007-9098-2

Reddad Z, Gerente C, Andres Y, Pierre LC (2002) Adsorption of several metal ions onto a low-cost biosorbent: kinetic and equilibrium studies. Environ Sci Technol 36:2067–2073

Sheshdeh RK, Nikou MRK, Badii K et al (2014) Equilibrium and kinetics studies for the adsorption of Basic Red 46 on nickel oxide nanoparticles-modified diatomite in aqueous solutions. J Taiwan Inst Chem Eng 45:1792–1802. https://doi.org/10.1016/j.jtice.2014.02.020

Sing K, Williams R (2004) Physisorption hysteresis loops and the characterization of nanoporous materials. Adsorpt Sci Technol 22:773–782. https://doi.org/10.1260/0263617053499032

Sun Z, Zhang Y, Zheng S et al (2013) Preparation and thermal energy storage properties of paraffin/calcined diatomite composites as form-stable phase change materials. Thermochim Acta 558:16–21. https://doi.org/10.1016/j.tca.2013.02.005

Vimonses V, Lei S, Jin B et al (2009a) Kinetic study and equilibrium isotherm analysis of Congo Red adsorption by clay materials. Chem Eng J 148:354–364. https://doi.org/10.1016/j.cej.2008.09.009

Vimonses V, Lei S, Jin B et al (2009b) Adsorption of congo red by three Australian kaolins. Appl Clay Sci 43:465–472. https://doi.org/10.1016/j.clay.2008.11.008

Wang S, Zhu ZH (2006) Characterisation and environmental application of an Australian natural zeolite for basic dye removal from aqueous solution. J Hazard Mater 136:946–952. https://doi.org/10.1016/j.jhazmat.2006.01.038

Wang Y, Mu Y, Zhao QB, Yu HQ (2006) Isotherms, kinetics and thermodynamics of dye biosorption by anaerobic sludge. Sep Purif Technol 50:1–7. https://doi.org/10.1016/j.seppur.2005.10.012

Wang B, de Godoi FC, Sun Z et al (2015) Synthesis, characterization and activity of an immobilized photocatalyst: natural porous diatomite supported titania nanoparticles. J Colloid Interface Sci 438:204–211. https://doi.org/10.1016/j.jcis.2014.09.064

Weber WJ, Morris JC (1963) Kinetics of Adsorption on Carbon from Solution. J Sanit Eng Div 89:31–60

Ye X, Kang S, Wang H et al (2015) Modified natural diatomite and its enhanced immobilization of lead, copper and cadmium in simulated contaminated soils. J Hazard Mater 289:210–218. https://doi.org/10.1016/j.jhazmat.2015.02.052

Yuan P, Liu D, Fan M et al (2010) Removal of hexavalent chromium [Cr(VI)] from aqueous solutions by the diatomite-supported/unsupported magnetite nanoparticles. J Hazard Mater 173:614–621. https://doi.org/10.1016/j.jhazmat.2009.08.129